CoA NOTE MAT. No. 12

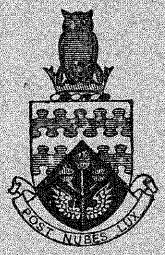

THE COLLEGE OF AERONAUTICS
CRANFIELD

THE EFFECT OF PLASTIC ANISOTROPY ON FLANGE WRINKLING BEHAVIOUR DURING SHEET METAL FORMING

by

H. Naziri and R. Pearce

CoA Note Mat. 12

THE COLLEGE OF AERONAUTICS

DEPARTMENT OF MATERIALS

The effect of plastic anisotropy on flange wrinkling behaviour during sheet metal forming

- by -

H. Naziri, D.A.E. and Roger Pearce, B.A., B.Sc., F.I.M.

C O R R I G E N D A

Page 2, Equations (3) and (4) should read:

$$0.46 \left(\frac{t}{b}\right)^2 \leq \frac{\sigma_c}{E_o} \leq 0.64 \left(\frac{t}{b}\right)^2 \qquad (3)$$

$$1.65 \left(\frac{a}{b}\right) \leq N \leq 2.33 \left(\frac{a}{b}\right) \qquad (4)$$

Page 6, paragraph 2, line 2 should read:

The mean cup-height $\frac{(h_e+h_t)}{2}$ where h_e and h_t are the heights of the ears

Page 9, equation (12) should read:

$$\frac{\sigma_x}{X} = \sqrt{\frac{2r+2}{2r+1}}$$

CoA Note Mat. 12

October, 1967

THE COLLEGE OF AERONAUTICS

DEPARTMENT OF MATERIALS

The effect of plastic anisotropy on flange wrinkling behaviour during sheet metal forming

- by -

H. Naziri, D.A.E. and Roger Pearce, B.A., B.Sc., F.I.M.

SUMMARY

During the drawing of sheet metal between a die and a blankholder, compressive hoop-stresses are developed which attempt to thicken or wrinkle the flange. Previous work on this behaviour has ignored any effects due to normal or planar plastic anisotropy. In this paper it is shown that the blankholder pressure necessary to suppress wrinkling increases with decreasing normal anisotropy (r) and increases with increasing planar anisotropy (Δr). The approximate plane strain conditions ($d\epsilon_z = 0$) operating in the flange can be simulated by an edge-notched tensile specimen and this simulation demonstrates the effect of texture hardening and softening upon flange wrinkling behaviour. The results obtained can be interpreted qualitatively by the use of anisotropic plasticity theory.

The speed of drawing also effects wrinkling, in general, the number of wrinkles decreases with increasing drawing speed.

Contents

The sheet metal forming process is usually terminated by the onset of instability, which can be tensile or compressive. In the tensile case, and in so-called deep-drawing, which is characterised generally by failure on or near the punch-profile radius, failure occurs in plane strain ($d\epsilon_y = 0$) (Figure 1) and the plastic strain ratio, r, is probably the most important material property. In stretch forming where $d\epsilon_x$, $d\epsilon_y$, $d\epsilon_z \neq 0$, a ductility parameter such as uniform or total elongation, or the work-hardening exponent, n, seems to be the parameter which correlates most closely with maximum strain instability. Bott and Pearce[1] have shown that r also has an effect in this situation.

The onset of compressive instability can also be a cause of failure, either because the shape requirements of the pressing are not achieved, or because the folding-up of the metal - an advanced form of compressive instability - results in the development of high forming loads which cause fracture elsewhere in the part. Compressive instability is variously termed buckling, folding, crinkling and wrinkling. The term 'buckling' is used - often expanded to 'body buckling' - to describe bad shape in the body of a pressing, whilst wrinkling is confined to the flange behaviour. It is this term in this connotation which will be used in the present paper.

Wrinkling has been treated by previous workers (2-7), both theoretically and experimentally. The first treatment was by Geckeler (2) who considered theoretically the case of drawing without a blankholder and treated the radial cross-section of the flange as a bar of length equal to the mean flange circumference, which, under the induced hoop stress, collapsed into a series of radially disposed wrinkles. He evaluated:-

(1) The critical compressive hoop-stress (σ_c) which would cause this to occur, viz.,

$$\sigma_c = 0.46 \frac{E_o t^2}{b^2} \qquad (1)$$

where E_o is the buckling modulus, t the metal thickness and b the width of the flange.

(2) The number of waves (N) into which the flange would collapse, viz.,

$$N = 1.65 \frac{a}{b} \qquad (2)$$

where a is the mean flange radius.

The first experimental investigation was that of Howald and Baldwin (3) using copper, 70/30 brass, various tempers of aluminium and a rim-steel and this work was later checked and expanded by Senior (5)(6), who replaced the rim-steel of the first investigation with an aluminium-stabilized steel.

Howald and Baldwin found good agreement between their experiments and Geckeler's theory, and concluded that the plastic properties of the material had little effect on wrinkling, except that aluminium and brass were slightly more prone to wrinkling than was predicted. Senior found a wider spread in results and introduced a transition region between wrinkled and wrinkle-free conditions, viz.

$$0.46 \left(\frac{t}{b}\right)^2 \geqslant \frac{\sigma_c}{E_o} \leqslant 0.64 \left(\frac{t}{b}\right)^2 \qquad (3)$$

Even though the number of wrinkles formed for various blank diameters was in reasonable agreement with the results of Howald and Baldwin, Senior afforded a similar treatment to Geckeler's second equation, viz.,

$$1.65 \left(\frac{a}{b}\right) \geqslant N \leqslant 2.33 \left(\frac{a}{b}\right) \qquad (4)$$

He further investigated constant clearance and constant load blank-holding and derived equations for N for those two conditions which fitted well with the experimental results. An anomaly in Senior's work is that in the case of the aluminium-stabilized steels, the theory overestimates σ_c, i.e., greater reductions are possible than those predicted, before wrinkling ensues. The work of Miwagawa (7) in general confirms that of previous workers, and does not introduce anything significantly new.

In general, these authors conclude that material properties, even elastic and tangent modulus, play little part in flange-wrinkling behaviour in comparison with geometrical and dimensional factors. However, as will be shown later, conditions exist where experimental results do not agree with theories based simple on geometrical and dimensional factors and material properties must be considered.

In this work the effect of anisotropy on flange wrinkling has been studied. Isotropy in all sheet metal whether commercially or experimentally produced is the exception rather than the rule. One parameter for the characterization of anisotropic plastic properties is the strain ratio

$$\frac{d\epsilon_x}{d\epsilon_z}$$

measured in uniaxial tension, and usually termed the $\underline{r}$-value.* The $\underline{r}$-value varies in the plane of the sheet and a parameter Δr is used as a measure of planar anisotropy. Δr is related to the earing behaviour of a metal (8). The present work was initiated by empirical observations of the apparent resistance to flange wrinkling of certain steels with average $\underline{r}$-values greater than unity. A systematic study was then made of the behaviour of materials a range of $\underline{r}$ and $\Delta\underline{r}$ values and the results interpreted using anisotropic plasticity theory (9,10).

---

* r average $= \bar{\underline{r}} = \dfrac{r_o + 2r_{45} + r_{90}}{4}$

Materials

The materials used in this investigation were as follows:

1. Steel

Copper-containing extra-deep-drawing steel, 0.036-in., thick 'Jouvencel' ex- S.A. Metallurgique d'Esperance-Longdoz, ex- Copper Development Association.

2. Aluminium

Commercial-purity aluminium 0.036-in. thick coil, ex Alcan Industries Ltd.

3. Zinc

0.25-in. Commercial-purity zinc plate, rolled to 0.036-in. thickness before drawing, ex RTZ Ltd.

4. Titanium

0.036-in. thick titanium 115 ex IMI (Kynoch) Ltd.

Experimental Procedure

Most of the apparatus used in the tests is standard equipm nt and has been previously described (1).

The experimental procedure can be conveniently subdivided into two parts:

1. Fundamental tests (uniaxial tensile and plane strain [$d\epsilon_z = 0$] notch)

Duplicate tensile test specimens having overall lengths of about 6.5 in. and a width of 0.5 in. over a parallel length of 2.5 in. were used. To observe directionality the tensile-test specimens were cut with their axes at 0°, 45° and 90° to the direction of rolling of the sheet. From these specimens proof strength, tensile strength and strain ratio (see Table 1) were determined.

The required vee-notches were cut in the edges of 0.75-in. wide strips; the notch dimensions are quoted in Table 2. From these specimens values of the flow stress at various strains (see Table 2) were obtained. A Hounsfield extensometer was used for the strain measurement in this part of the investigation.

2. Simulative tests (flange wrinkling)

Deep drawing press and tooling.

Individual flat-bottomed punch and die sets were attached to a 35-ton-maximum-load, Hille-Engineering press, equipped with an X-Y recorder to record load versus punch travel. Since the press was not capable of providing a blank-holder pressure (constant load) of less than 60 p.s.i. a hydraulic piston and cylinder unit was attached to the blankholder pressure transmitting unit on the machine. With this attachment it was possible to obtain blankholder pressures as low as 25 p.s.i. by the application of dead weights. The die set and flat-bottom punch gave a nominal 2-in. diameter cup, self-centering fingers were used to locate the blanks.

The constant-load blankholder pressure was hydraulically transmitted onto the blank surface by means of a pressure plate, which, when the blankholder (constant load) was not employed, acted as a constant-clearance blankholder up to a maximumclearance of 0.25 in. This could be reduced, if required, such that there was zero clearance between the die and pressure plate. The depth of partially-formed cups was measured by means of a dial gauge (least count 0.001 in.), and another dial gauge was appropriately mounted to indicate any increase in clearance caused by the deflection of the tools during the drawing operation. When no blankholder was required the pressure plate was removed. The blanks could then be placed on the punch, and pressed into the die to the required depth of punch travel.

Simulative flange-wrinkling tests.

To standardise the blank diameter, it was necessary that all the metals under consideration could be drawn successfully into a flat-bottomed cylindrical cup. Preliminary tests showed that the largest blank which could be drawn successfully for zinc, the lowest $\bar{r}$-value metal in this study, was 4 in. Thus, in all the flange-wrinkling tests, 4 in. diameter blanks were used. The blanks were cut oversized and machined to size using a slow cutting-speed to minimize any edge work-hardening effects. All blanks were 0.036 in. $\pm$ 0.002 in. thickness. A punch speed of 0.61 ft/min. was used in most cases, but a speed of 39.4 ft/min. was also used.

Measurement of ear and trough heights.

The simple set-up shown in Fig. 2 was used to measure the ear and trough heights of the cupped blank. The cup was inserted into the ring resting on a gauge plate, and the three Allen screws on the periphery of the ring were used to centralise and clamp the cup. The V-ended spindle of a dial gauge (least count 0.001 in.) was brought into contact with the rim and the ring, with the cup, rotated. Readings of the dial gauge were noted to evaluate the ear and trough heights.

Detection of the commencement of wrinkling without a blankholder.

Blanks were scribed with diametrical lines at 5° intervals. These were

mounted on the fixture shown in Fig. 3. The blanks were rotated by means of the spindle and the wave amplitude noted. The blanks were then drawn by increments of 0.01 in. and after each draw, the partially-drawn blank re-mounted on the fixture and rotated to determine the magnitude of the wrinkling.

Lubrication.

As friction between the blank and the tool surfaces can produce considerable variations in the results of simulative tests, it was necesssary to adopt a standard lubrication procedure in this investigation. Polyethylene film, 0.0015-in thick was employed on both sides of the blank, cut away to allow the punch nose to remain in contact with the sheet metal. This lubrication system, by eliminating metal to metal contact between the die and blankholder and the blank prevented any variations in the surface finish of the sheet metal from having an effect upon the experimental results. By allowing contact between the blank and the punch negligible straining occurred over the punch nose and punch profile radius, and so a condition akin to pure deep drawing was obtained. Finally, this set of conditions allowed the successful drawing of four-inch diameter zinc-blanks, which would have been difficult under other lubrication conditions.

The results of the initial tests, carried out to determine the simulative testing procedures, showed that no increase in drawing load occurred with increasing blankholder pressure over the range 60-850 lbs., though an increase in the ironing component is observed (Figure 4). The reason for this is that the extremities of the ears which, late on in the draw, must protrude slightly from the polyethylene film, are nipped between the die and the blankholder, and thinned. Examination of the cups reveals increased thinning with increasing blankholder pressure, consequently an increased load is recorded. Figure 5 shows the effect of lubrication on cups drawn at 300 lbs blankholder pressure. An increase in cup-rim irregularity without lubrication is demonstrated in Figure 6, while a study of the cup wall shows that a more parallel wall is achieved without lubrication; clearly, friction is 'sticking' the blank to the punch and providing a better-shaped part. Figure 5 also shows a fall in the maximum drawing load with the addition of TSD 996 - a mineral oil - to both sides of the polyethylene film. However, with the lack of any systematic investigation of the effect of oil on polythene lubrication, dry polyethylene film, applied as previously described, was used.

Results

The uniaxial properties and the blankholder pressure required to suppress wrinkling are given in Table 1. The modulus values are taken from various sources - the proof strengths and tensile strengths are not anomalous and do not require comment. The strain ratios agree in general with previously measured values, though in the case of titanium, r_{90} is seen to be strain-dependent. However $\bar{r}$ shows a value of approximately 4 for the three strains used. The loads required to suppress wrinkling are quoted in the last column; with the exception of zinc, this load decreases with increasing $\bar{r}$.

Effects due to normal anisotropy

The effect of different depths of punch penetration upon wrinkle-formation in zinc and steel is shown in Figure 7. In the case of steel ($\bar{r}$ = 1.50) the blank was not flat at the start of the test, but the wrinkle-amplitude was virtually unchanged at 0.14-in. punch penetration, while zinc ($\bar{r}$ = 0.35) which was initially flat, wrinkled considerably. When a full set of wrinkles had been developed, using a punch speed of 0.61 ft/min the number was invariably seven, in good agreement with Geckeler's prediction of 6 - 8 for the tool and blank dimensions employed in the present investigation. However, due to the experimental difficulties associated with lack of flatness, this approach was abandoned and the load required to suppress wrinkling in the range of materials used was determined, the results are listed in table 1. The load decreases with increasing $\bar{r}$ except in the case of zinc. From other results (11) the plastic deformation of commercial-purity zinc is thought to be anomalous, and this result is thus not unexpected.

The value of $\bar{r}$ has an effect on final cup-height as shown in Figure 8 The mean cup-height $\frac{(h_e - h_t)}{2}$ where h_e and h_t are the heights of the ears and the troughs respectively, was plotted against $\bar{r}$ and it was found that, for a given blank diameter, the mean cup-height increases with increasing $\bar{r}$.

Effects due to planar anisotropy ($r = 1, \Delta r \neq 0$)

For round blanks of zinc, aluminium, aluminium-stabilized steel drawn without a blankholder at 0.61 ft/min. seven wrinkles were observed as previously described for the rotationally symmetrical case. However, at the higher speed of 39.4 ft/min a different effect was observed as illustrated in Figure 9 in that zinc showed two wrinkles, while aluminium and steel each showed four. This is remeniscent of the earing behaviour of these metals (same figure) and suggests that, at higher drawing speeds, wrinkling occurs at positions of low r-value. Square blanks were also drawn. For zinc, rotation of the blank relative to the rolling direction through 45° altered the number of wrinkles from 2 to 4 (Figure 10) while cutting out the blank in different orientations had no effect on the wrinkles developed in steel and aluminium both of which show four symmetrical ears (Figure 11). In the case of titanium four equal wrinkles developed when r = 3.3 was put in the centre of the sides, but two deep and two shallow wrinkles resulted from 45° rotation (Figure 12). This is intermediate between the two-wrinkle case of zinc and the four-equal-wrinkle cases of aluminium and steel. The reason for this is made clear in Figure 13. Wrinkling will not occur on the diagonals, for the hoop stress is zero at the extreme corner and, travelling inwards from this point, any other point is restrained from buckling by the triangular tab consisting of the corner of the square. Similar effects are observed with constant-clearance and constant-load blankholding (Figure 14).

Variations in Δr may be achieved by cross rolling, without variation

in the total amount of cold reduction. In this way the effect of Δr on the blankholder pressure required to suppress wrinkling may be seen (Figure 15); it is evident that, with the two metals tested, the greater Δr the greater the required blankholder pressure.

Discussion

The present work has shown that flange wrinkling behaviour depends on both normal and planar anisotropy, in contrast to previous work, in which the elastic modulus and the tangent modulus were the only material properties thought relevant to this form of instability. Geckeler's equations may be rewritten:

$$\sigma_c = KE_o = k' \frac{4E\ T_m}{(E+\sqrt{T_m})^2} = \frac{4E\ T_m}{(\sqrt{E}+\sqrt{T_m})^2}$$

and so $$\sqrt{\sigma_c} = k'' \frac{\sqrt{E}\sqrt{T_m}}{\sqrt{E}+\sqrt{T_m}} \qquad (5)$$

where E is the elastic modulus of T_m the tangent modulus.
Plotting $\sqrt{\sigma_c}$ against $\sqrt{E}$ or $\sqrt{T}$ gives a curve of the form shown in Figure 16 where the asymtote is $K\sqrt{E}$ or $k\sqrt{T_m}$ respectively.

Plotting σ_c should increase with increasing E and increasing T_m. Table 2 shows quoted values for E and measured values of the ratio tensile strength to 0.1% proof strength (T/Y) for all the materials tested. This latter is a measure of the slope of strain-hardening portion of the load/extension curve and decreases with increasing n (where $\sigma = A\epsilon^n$) or T_m. Thus materials with high E and high T_m (or T/Y) should give high values of σ_c and so increased resistance to wrinkling. Alternatively, the factor E x T/Y should be as high as possible. It can be seen that predictions based on this model do not fit the experimental results. However, Pearce (12) has shown that the ratio Y/T is important in the case of body buckling in ageing temper-rolled rim-steels.

A better model for wrinkling can be constructed using anisotropic plasticity theory and the concepts of texture hardening and softening. The von Mises yield-criterion predicts yielding in the special case of an isotropic material ($r = 1$, $\Delta r = 0$) when:

$$(\sigma_z-\sigma_x)^2 + (\sigma_x-\sigma_y)^2 + (\sigma_y-\sigma_z)^2 = 2X^2 \qquad (6)$$

where X is the yield stress in uniaxial tension.

This relationship is usually shown graphically for the plane stress condition, $\sigma_z = 0$, where it plots as an ellipse of the form

$$\sigma_x^2 - \sigma_x\sigma_y + \sigma_y^2 = X^2. \qquad (7)$$

Hill's generalization for the anisotropic case predicts yielding when

$$F(\sigma_y-\sigma_z)^2 + G(\sigma_z-\sigma_x)^2 + H(\sigma_x-\sigma_y)^2 = 1, \qquad (8)$$

where F, G and H are anisotropic stress parameters, and this reduces to:

$$\sigma_x^2 - (\frac{2r}{r+1})\sigma_x\sigma_y + \sigma_y^2 = X^2 \qquad (9)$$

for the case of rotational symmetry about the z axis, and has been applied in the present work.

Recently Hosford (13) has proposed a more general relationship for plane-stress loading, namely:

$$P(R+1)\sigma_x^2 - 2RP\sigma_x\sigma_y + R(P+1)\sigma_y^2 = P(R+1)X^2 \qquad (10)$$

where R can be equated to the average strain ratio ($\bar{r}$) as defined in this paper (10).

Equation (6) plots as an ellipse having the major axis at 45° to the origin of the orthogonal co-ordinates on which it is constructed, while equation (7) with increasing r-values, stretches out the ellipses in the tension - tension quadrants and pulls in the ellipses in the tension compression quadrants, preserving their symmetry with regard to the original axes. The stretching out and pulling in of yield loci by anisotropy is respectively termed texture hardening and softening. For the more general case (eq. 10) with $\Delta r \neq 0$ or, as stated by Hosford $R \neq P$, the major axis of the ellipse is rotated away from 45° to the origin.

Any attempt to draw a cup from sheet metal without applied blankholder pressure will result inevitably in wrinkling and can be therefore considered as a series of bending operations with $d\varepsilon_y = 0$. This plane strain situation is represented in the first quadrant by the loading path

$$\frac{r}{r+1}$$

and thus increasing r values will give resistance to bending and hence wrinkling. When the flange of a cup is confined between die and blankholder it is under a stress system giving rise to plane strain with $d\varepsilon_z = 0$, ignoring the tendency to thicken at the rim. The loading path is represented by $\alpha = -1$ in the second quadrant of the plane stress loci of figure 7. Again, a high r-value material, which here possesses a lower flow stress than a low r value material, will resist wrinkling by deforming more readily in the sheet plane due to texture softening. Crystallographically, a high r-value material is one in which the majority of the operating slip systems lie in the plane of the sheet. The resistance to bending and wrinkling

represented in the tension - tension quadrant and the deformation in the plane of the sheet under imposed blankholder pressure is thus simply explained. The tendency to wrinkle will be greater in low r-value material, and a greater blankholder pressure will be required to suppress it. In the present work the results for aluminium and titanium should be compared. A similar localized effect would be expected preferentially in the regions of low r-value in a metal exhibiting planar anisotropy, and this was found in the present work. It will be noticed in Figure 18 that the zinc blank has wrinkled in the low-r regions long before any significant geometrical changes have ensued which might be invoked as an alternative explanation for this phenomenon.

Hosford and Backofen have calculated various values of the larger principal stress relative to the uniaxial yield stress, and those relevant to the flange are given below. For the stress ratio $\alpha = -1$

$$\frac{\sigma_x}{X} = \sqrt{\frac{r+1}{2r+1}} \qquad (11)$$

so for increasing r, $\frac{\sigma_x}{X}$ decreases, i.e. the flow stress in the sheet plane decreases. For the case of an edge-notched strip, which relates also to the strength of material in a cup-flange deforming in plane strain, the relationship is

$$\frac{\sigma_x}{X} = \sqrt{\frac{2r+2}{2r+1}} \qquad (12)$$

which gives twice the value for $\frac{\sigma_x}{X}$ though producing a curve of $\frac{\sigma_x}{X}$ vs. r of similar form. Strictly, the loading path here does not lie in Figure 17 for σ_y is now zero and there is a stress σ_z. The measured values of $\frac{\sigma_x}{X}$ in this work, however, fit better with the latter relationship, so this is used for the curves in Figure 19, which are plotted from the data in Table 2, which gives the range of notch dimensions tried. A notch depth of 0.163 ins. with anotch angle of 90° proved the most satisfactory and the strains developed are clearly similar in the two cases.

Conclusions

1. Previous work on wrinkling which ignores anisotropy does not explain the observed phenomena.

2. For anisotropic materials ($r \neq 1$, $\Delta r = 0$, $\Delta r \neq 0$) which are deformed slowly, Geckeler's equation predicts the observed number of wrinkles.

3. At higher punch speeds, with metals showing $\Delta r \neq 0$, the flange forms a

number of wrinkles equal to the number of ears which would finally form on a drawn cup; this number represents the low r-value regions of the blank and is not predicted by Geckeler's equation.

4. Blankholder pressure required to suppress wrinkling increases with decreasing r value.

5. Blankholder pressure to suppress wrinkling increases with increasing Δr, suggesting the minimum r-value as the critical parameter.

6. Texture hardening and softening provide an adequate qualitative explanation for all these phenomena.

7. The experimental relationship between $\frac{\sigma_x}{X}$ and r for an edge-notched test piece is shown to give a reasonable fit with the theoretical relationship $\frac{\sigma_x}{X} = \sqrt{\frac{2(r+1)}{2r+1}}$.

References

1. Bott, C.H., and Pearce Roger — The effect of varying strain-ratio on the hydraulic bulging behaviour of aluminium sheet. The College of Aeronautics Note Mat. No. 9.

2. Geckeler, J.W. — Plastic folding of the walls of hollow cylinders and some other folding phenomena in bowls and sheets. Z angew, Math. Mech. 1928, 8 341.

3. Howald, T.S., and Baldwin, W.M. — Folding in the cupping equation. Trans. A.S.M. 1947 38 757.

4. Sanders, J.S., and Loxley, E.M. — Wrinkling during cylindrical drawing operations. BISRA report MW/E/37/52.

5. Senior, B.W. — Flange wrinkling in the cup drawing operation with no blankholding. BISRA report MW/E/45/53.

6. Senior, B.W. — Flange wrinkling in deep drawing operations. J. Mech. Phys. Solids 1955-57 4-5 23.

7. Miyagawa

8.	Wright, J.C.	The phenomenon of earing in deep drawing. Sheet Metal Industries 1965 42 814.
9.	Hill, R.	Mathematical theory of plasticity. O.U.P. 1950.
10.	Hosford, W.F. Jr. and Backofen, W.A.	Strength and plasticity of textured metals. Proceedings of the ninth Sagamore ordnance materials research conference. Syracuse University Press 1965.
11.	Williams, D.A.C.	The investigation of a ductility phenomenon in commercial-purity zinc. The College of Aeronautics Thesis 1967.
12.	Pearce Roger	Use of the Swift-cupping press for the assessment of steel sheet for cold pressing. Sheet Metal Industries 1960 37 647.
13.	Hosford W.F. Jr.	Texture strengthening. ASM Metals Eng. Quart. 1966 6 13.

TABLE 1

Metal	Modulus of Elasticity (E) x 10^6 psi	Proof Strength (r) at 0.1% elongation x 10^3 psi				Tensile Strength (T) x 10^3 p.s.i.				T_m/Y_m	$\frac{T_m}{Y_m}$ XE	Strain Ratio r				Blankholder Pressure Required to Suppress Wrinkling (p.s.i.)
		Y_o	Y_{45}	Y_{90}	Y_m	T_o	T_{45}	T_{90}	T_m			$20r_o$	$20\bar{r}_{45}$	$20r_{90}$	$20\bar{r}$	
Zinc commercial-purity	13	12.2	12.8	13.1	12.7	17.5	17.8	18.0	17.7	1.4	1.8	.275	.385	.390	.357	35
Aluminium commercial-purity	10	3.1	3.3	3.2	3.2	9.4	9.7	9.7	9.6	3.0	30.0	.690	.610	.660	.642	60
Aluminium - stabilised steel	28	20.6	22.6	22	21.7	39.2	43.5	43.3	42.0	2.0	54	1.85	1.35	2.00	1.64	55
Copper rim-steel		20.1	21.1	21.0	20.7	39.4	40.0	39.3	39.6			1.64	1.33	1.67	1.50	40
Titanium, commercial purity	15	37.8	43.8	47.9	43.20	54.0	54.8	55.8	54.9	1.3	19	$5r_o$	$5\bar{r}_{45}$	$5r_{90}$	$5\bar{r}$	35
												3.37	3.37	6 05	4.04	
												$10r_o$	$10\bar{r}_{45}$	$10r_{90}$	$10\bar{r}$	
												3.39	3.41	5.68	3.97	
												$15r_o$	$15\bar{r}_{45}$	$15r_{90}$	$15\bar{r}$	
												3.83	3.29	5.32	3.90	

a_{r_b} = (where a = measured at per cent elongation
b = angle to the direction of rolling)

TABLE 2

Notch Dimensions		$\sigma x/x$ at per cent elongation								
		Zinc commercial purity			Aluminium - Stabilised Steel			Titanium Commercial purity		
Angle ($\theta°$)	W in	.0025%	.005%	.01%	.0025%	.005%	.01%	.0025%	.005%	.01%
60	0.250	2.15	2.35	2.40	-	-	-	2.00	1.85	-
60	0.425	-	-	-	1.34	1.36	1.35	1.50	1.40	1.22
90	0.250	2.15	2.35	2.40	1.375	1.40	1.50	-	-	-
90	0.425	1.93	1.92	1.87	1.50	1.42	1.38	1.375	1.280	1.160

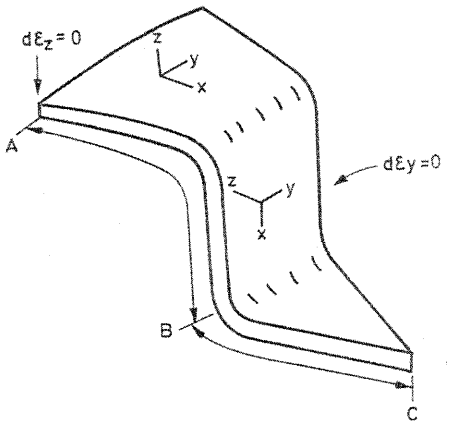

FIG. 1.

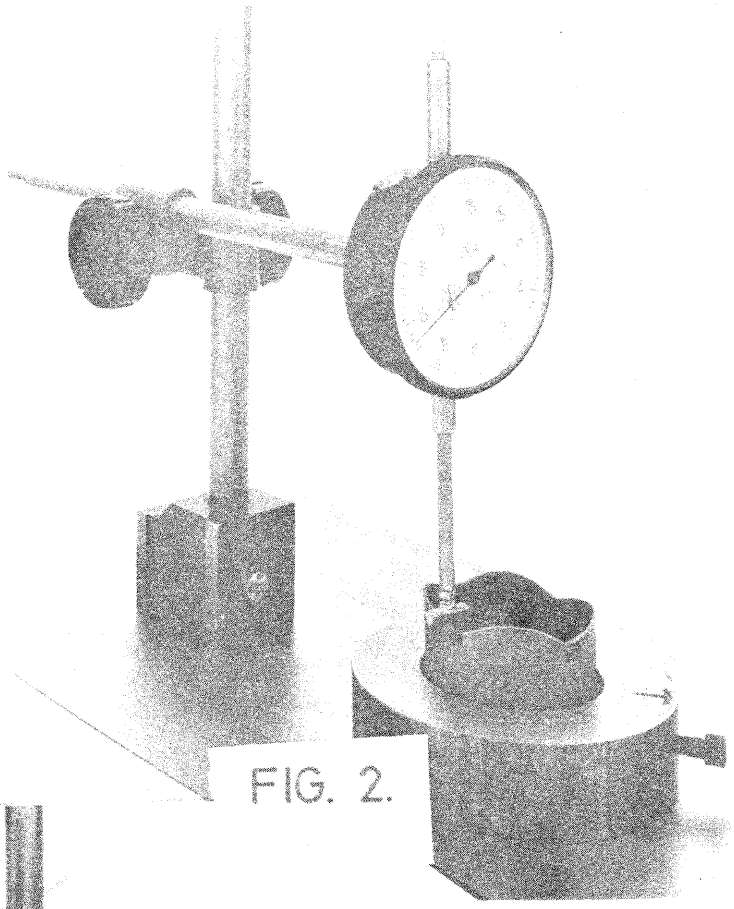

FIG. 2.

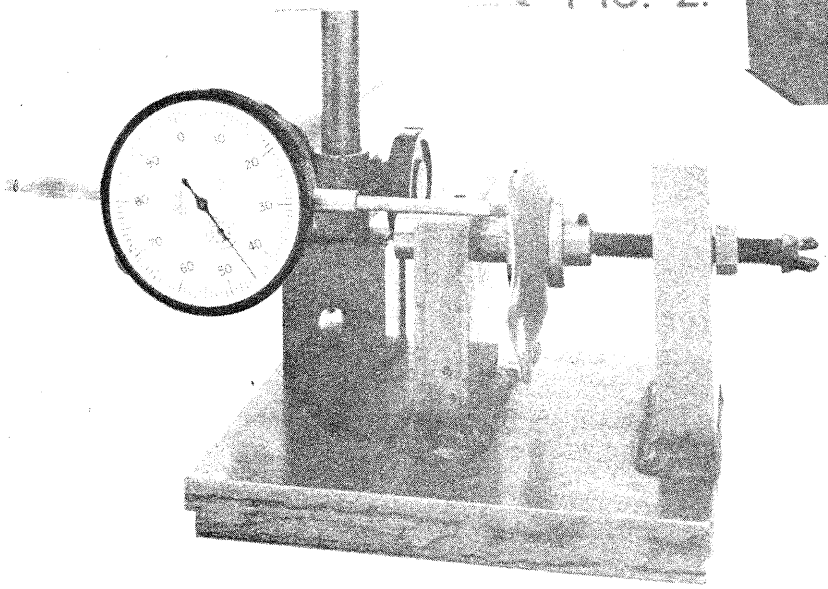

FIG. 3.

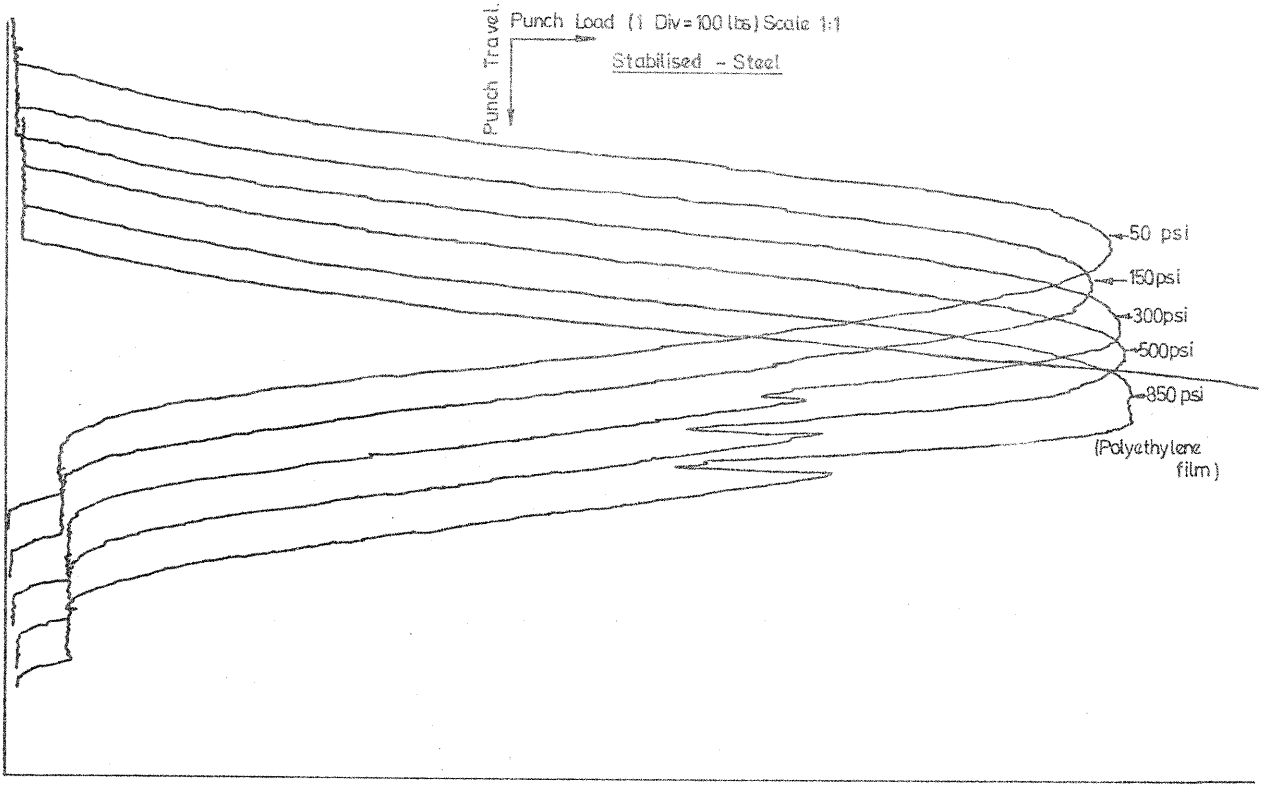

FIG. 4. EFFECT OF BLANKHOLDER PRESSURE ON PUNCH LOAD.

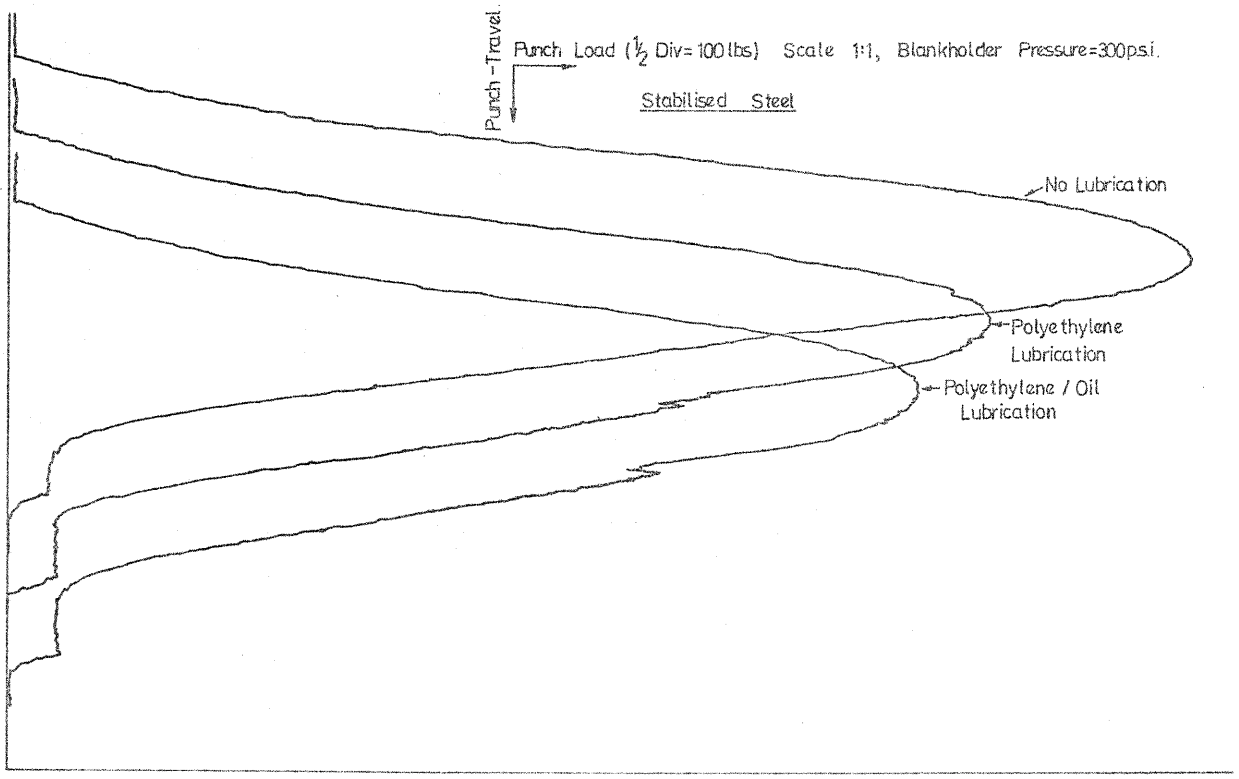

FIG. 5. EFFECT OF LUBRICATION ON PUNCH LOAD.

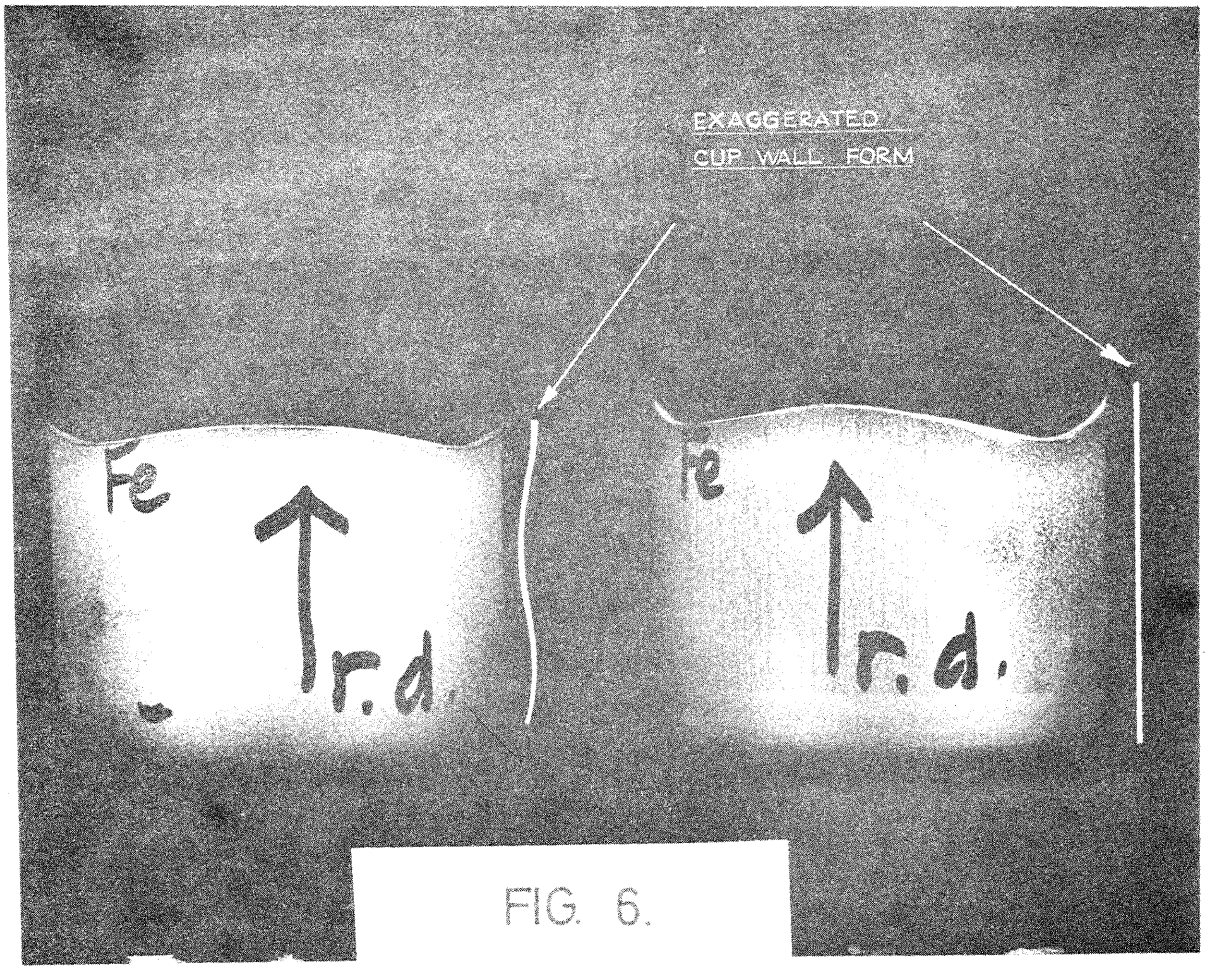

FIG. 6.

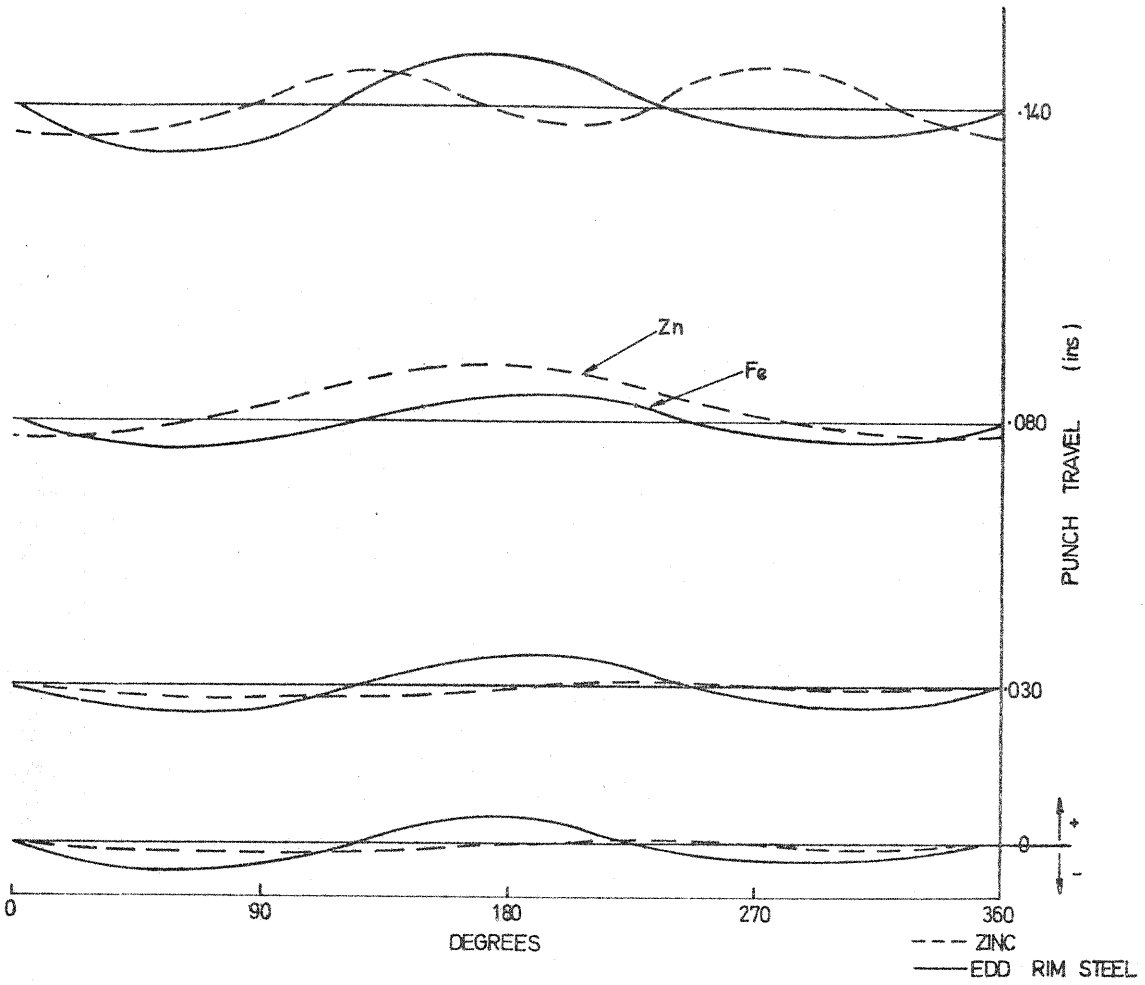

FIG. 7. WAVE AMPLITUDE AT DIFFERENT PUNCH TRAVELS.

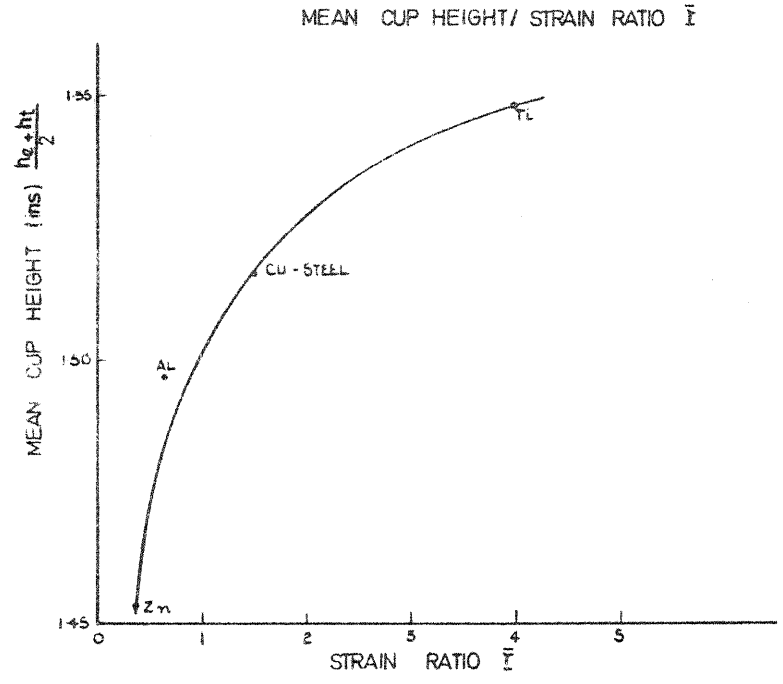

FIG.8

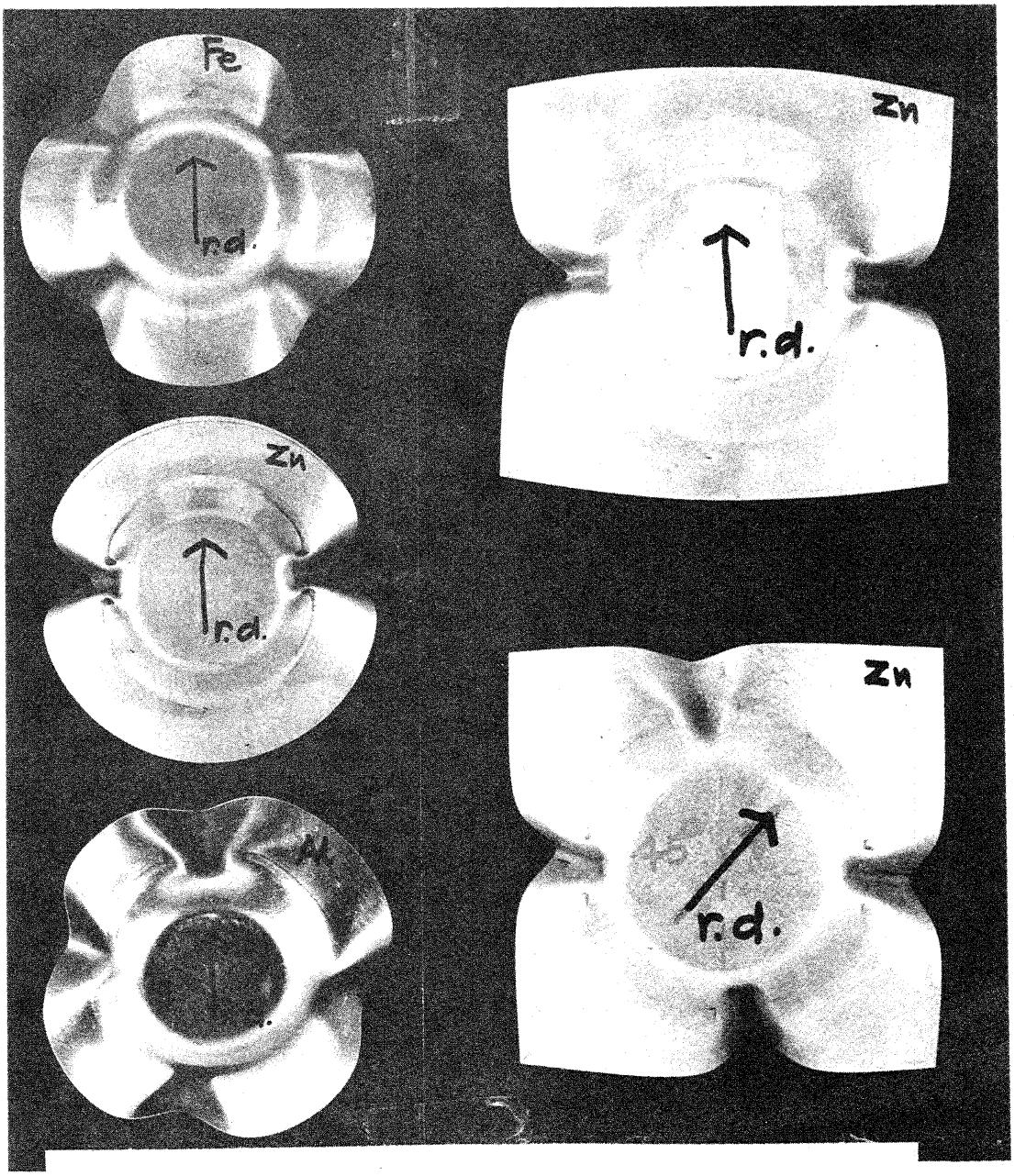

FIG. 9.

FIG. 10.

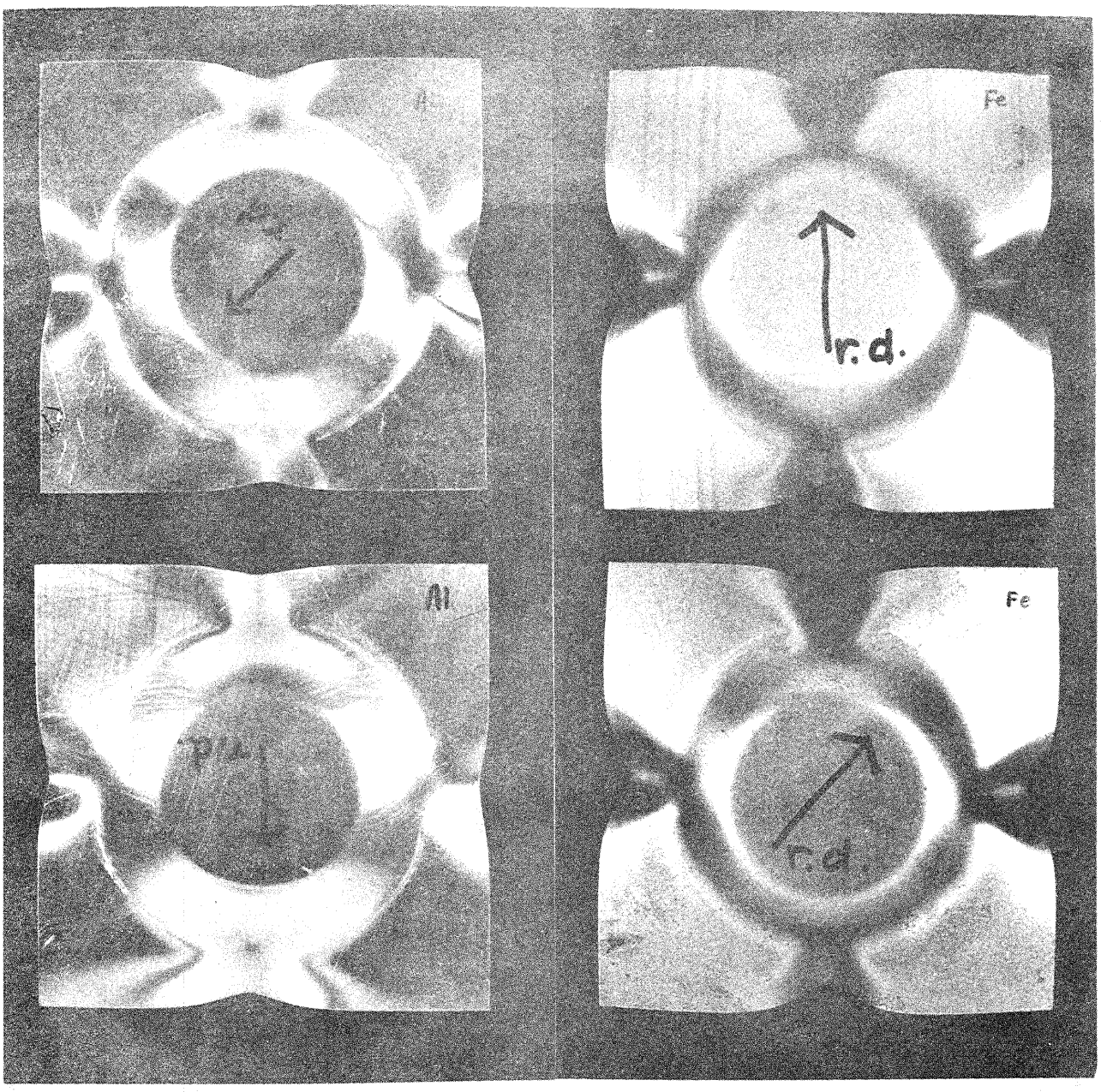

FIG. 11.

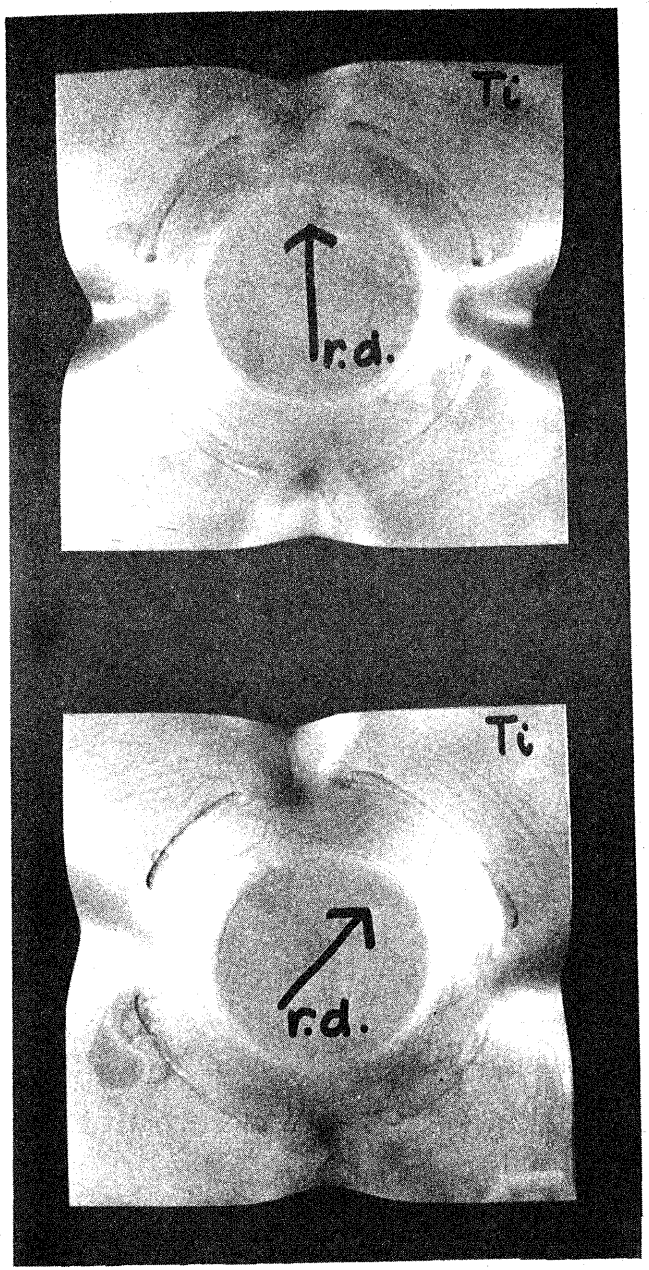

FIG. 12.

$\sigma_1 > \sigma_2 > \sigma_3 > \sigma_4 = 0$

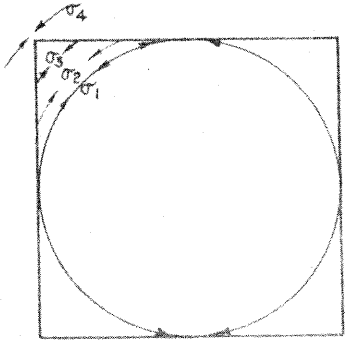

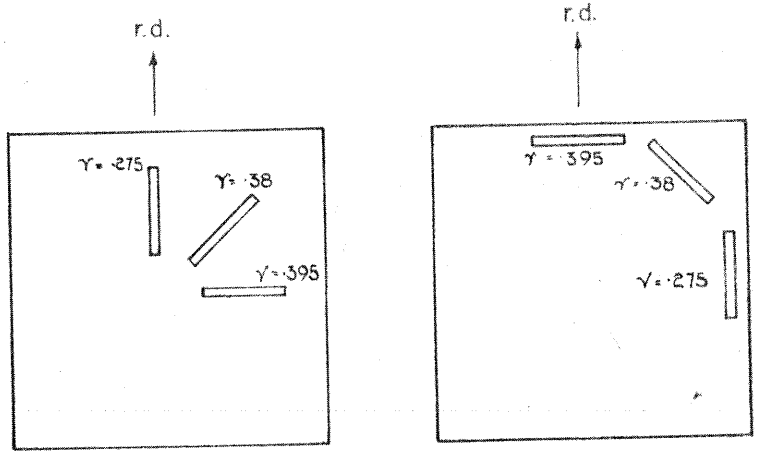

FIG. 13.

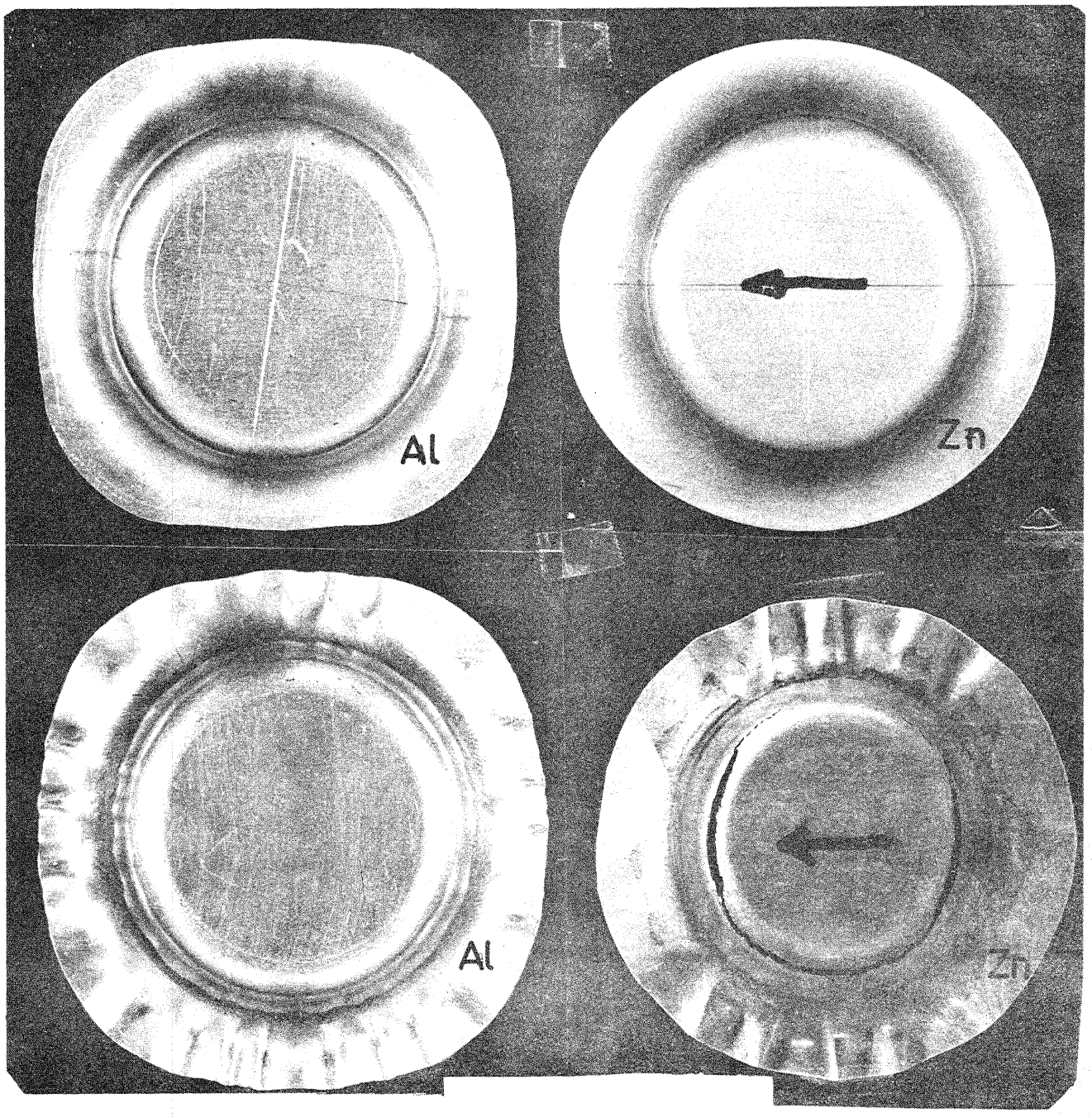

FIG 14.

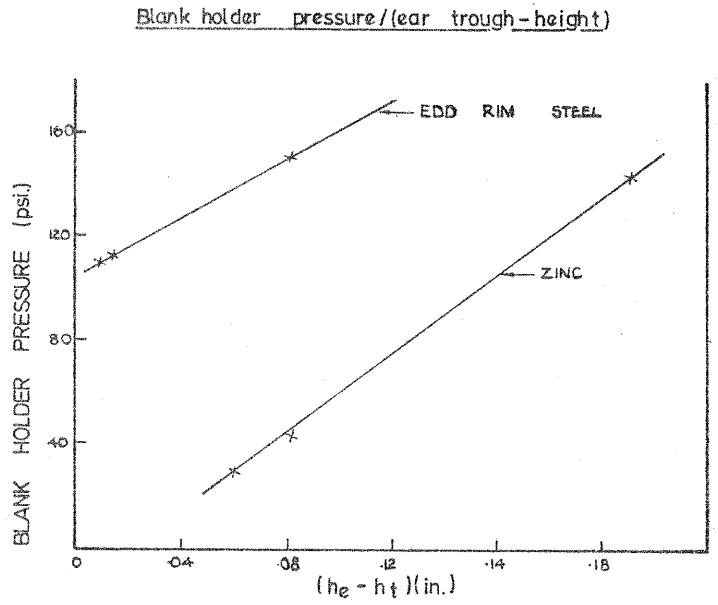

FIG. 15.

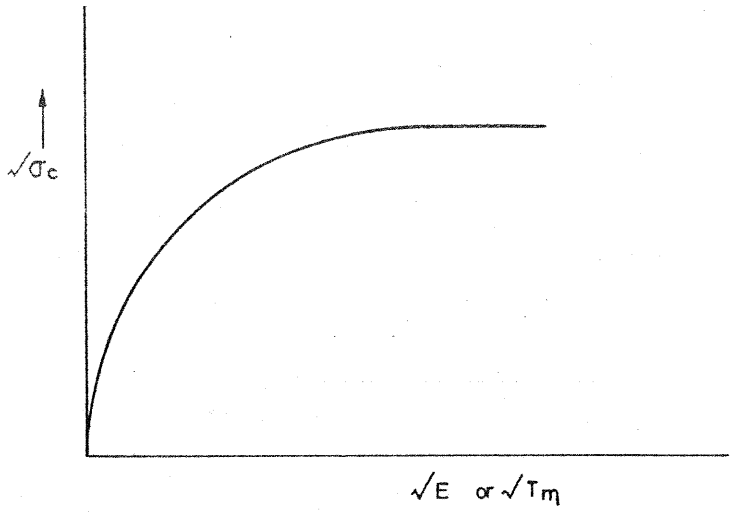

FIG. 16.

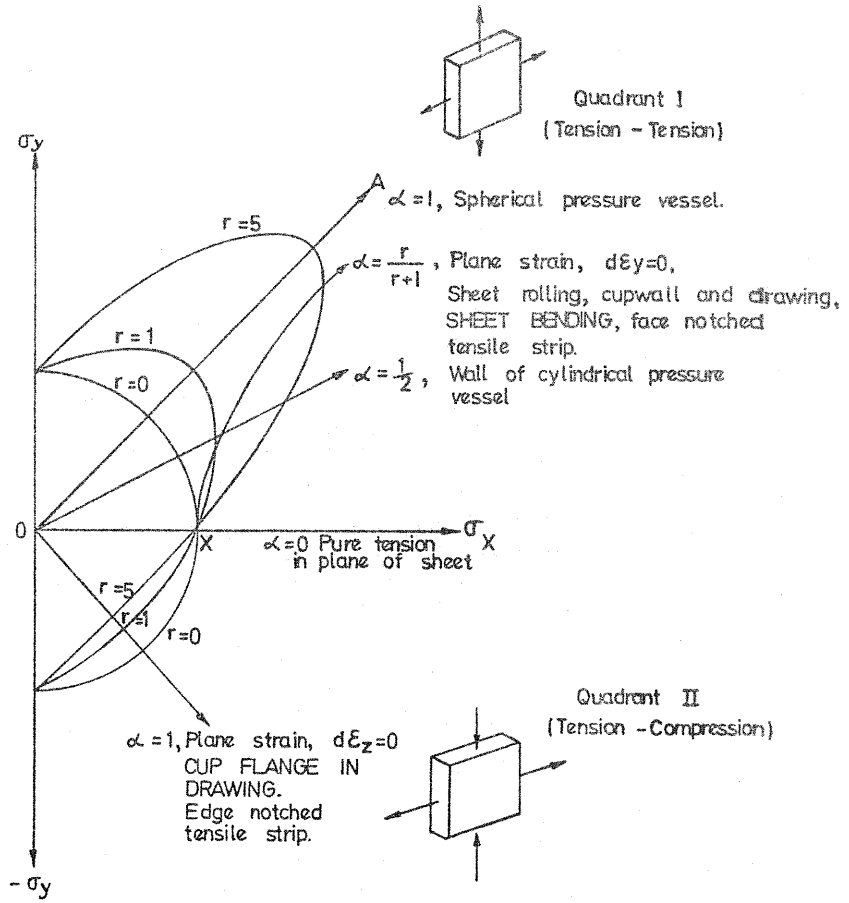

FIG. 17. PLANE STRESS YIELD LOCI.

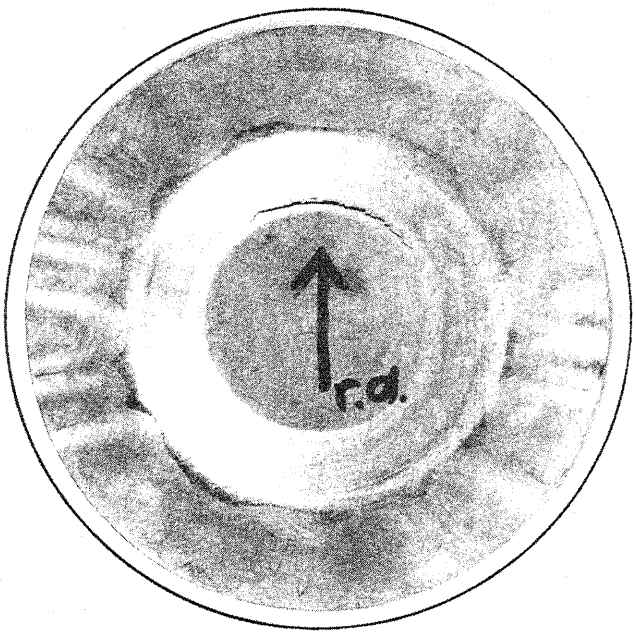

FIG. 18.

$$\frac{\sigma_x}{x} = \sqrt{\frac{2(r+1)}{2r+1}}$$

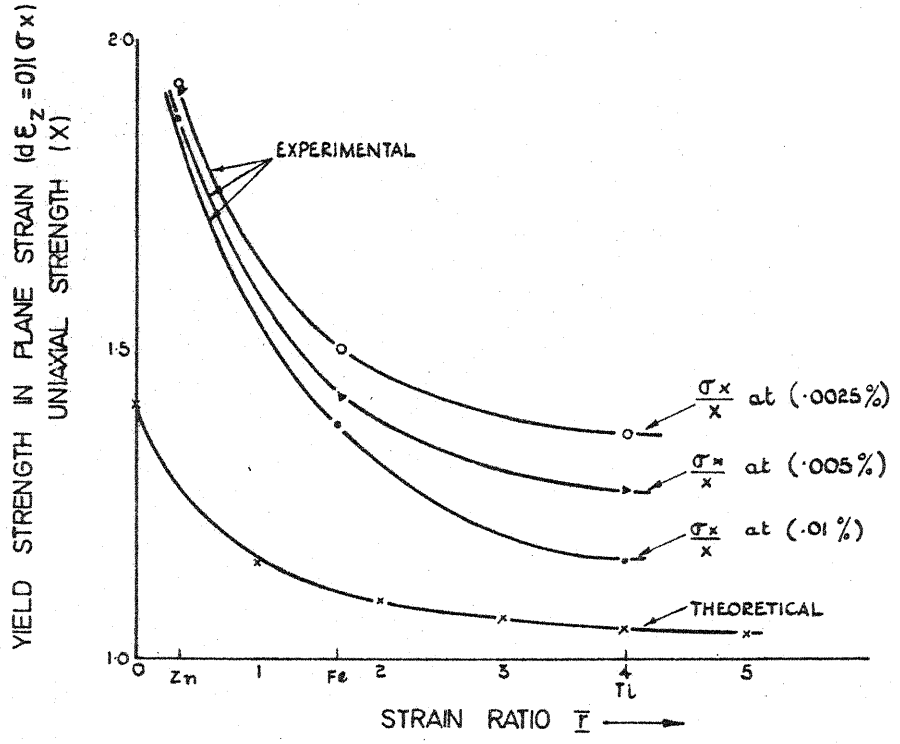

FIG19.